

Structure of a 2° (010) Cu twist boundary interface and the segregation of vacancies and He atoms

Enrique Martínez,* John P. Hirth, Michael Nastasi, and Alfredo Caro

Los Alamos National Laboratory, Los Alamos, New Mexico 87545, USA

(Received 31 October 2011; revised manuscript received 15 December 2011; published 7 February 2012)

A 2° (010) Cu twist boundary is characterized by two sets of $\frac{1}{2}\langle 110 \rangle$ screw dislocations crossing at misfit dislocation intersections (MDIs). Molecular dynamics simulations show that between MDIs, dislocations split into the two possible $\{111\}$ planes that share the $\langle 110 \rangle$ direction, forming a constriction where the glide planes change. Elasticity theory predicts the relative stability of such structures compared to structures without constrictions. Constrictions offer vacancy trapping sites that are lower in energy than those at the MDIs and with larger basins of attraction. For the substitutional He atom, MDIs and constrictions are comparable in energy. An off-lattice kinetic Monte Carlo code accounting for the presence of dislocations and their distortion fields shows that voids would form at the constriction points rather than at the MDIs. High-resolution experiments are needed to test the predicted structure.

DOI: [10.1103/PhysRevB.85.060101](https://doi.org/10.1103/PhysRevB.85.060101)

PACS number(s): 61.80.Az, 68.35.Dv, 61.72.J-, 66.30.Lw

Interfaces are well-known point defect sinks.^{1,2} Under irradiation, these defects and their clusters are created during collision cascades. Many deleterious effects of irradiation on material properties, such as void swelling and radiation-induced hardening and embrittlement, are due to the formation of these defects. The atomic structure at the interfaces characterizes the response to irradiation along with the mechanical properties, diffusivities, and susceptibilities to embrittlement.^{3–6} Recent advances in experimental techniques such as aberration-corrected transmission electron microscopy and atom probe tomography, coupled to the development of theoretical models and algorithms, have given control over this interface atomic structure. The goal is to tune the microstructure in such a way that defects annihilate themselves and therefore the system self-heals and withstands higher irradiation doses. Nanocrystalline materials and nanoscale foams show promise as radiation-tolerant structures due to their large sink densities.^{7–9} Twist boundaries (TBs) in particular provide a forum for models and experiments to test these ideas.

A (010) TB in fcc crystals is characterized by two perpendicular sets of $\frac{1}{2}\langle 110 \rangle$ screw dislocations. Most of the previous work on modeling twist interfaces in Cu and Cu alloys was carried out for twist angles larger than 2° .^{10–14} Analysis of these structures reveals perfect dislocations forming the interface, due presumably to the small distance between misfit dislocation intersections (MDIs). The interaction energy between a vacancy and the TB is most attractive at MDIs with values from -1.4 to -1.1 eV, with still negative values at the dislocation cores (around -0.5 eV).^{10,13} The trend seems to be the same for the substitutional He case, but with lower absolute values for the interaction energy, -0.35 eV at the MDI and approximately -0.25 eV at the dislocation cores.¹³ In this study we show how, for the 2° TB, perfect dislocations split into Shockley partial dislocations in a specific manner. This splitting modifies the atomic structure of the MDIs and the dislocation cores leading to different interaction values than the ones reported in the literature for perfect screw dislocations.

We have performed molecular dynamics (MD) simulations of a 2° (010) twist interface in Cu using the LAMMPS code¹⁵ with the Mishin *et al.* interatomic potential.¹⁶ The two grains

in the bicrystal are symmetrically misoriented 1° each along the y axis. The sample size is $12.28 \times 24.63 \times 12.28$ nm³ and periodic and constant-pressure boundary conditions were applied. Analysis of the resulting structure using a dislocation extraction algorithm¹⁷ (DXA) shows that the screw dislocations in this interface split into partials such that each half of the dislocation segment between two MDIs splits on a different $\{111\}$ plane, creating a constriction at the middle point where the gliding planes change (see Fig. 1). Additionally, MD reveals that this pattern is stable after annealing, suggesting a significant energy difference with respect to splitting into a single $\{111\}$ plane, as confirmed by dislocation dynamics (DD) calculations.

We report here the analysis of the energetics of the dislocation structure using a DD methodology accounting for partial dislocations and stacking-fault energies. The description of the algorithm to handle partial dislocations in DD is given in Ref. 19; its main feature is that the force due to the stacking-fault energy is accounted for in the right magnitude and direction independently of the character of the dislocation or the reactions it might undergo. Even though Cu is highly anisotropic and the DD implementation is based on linear isotropic elasticity, DD seems to capture the relative stability of the different interface configurations. In contrast, the MD simulations reflect both anisotropy and nonlinear elastic effects.

To check the stability of these dislocation constrictions using DD we have studied the configuration as given by MD and analyzed by the DXA. As described above, MD calculations were performed with fully periodic boundary conditions, currently unavailable in the DD code used in this study.¹⁹ We therefore use static nodes at the periphery of the network, where dislocations end. The initial and final configurations are shown in Fig. 2. The constrictions in the four dislocation segments at the center region are stable, while those at the other eight segments dissolve. The stability of the constrictions is related to the dislocation interactions at both the MDIs and the constriction itself. In this DD configuration the end points cannot be considered as MDIs and therefore there is an imbalance in the interactions that makes the formation of constrictions unfavorable. In contrast,

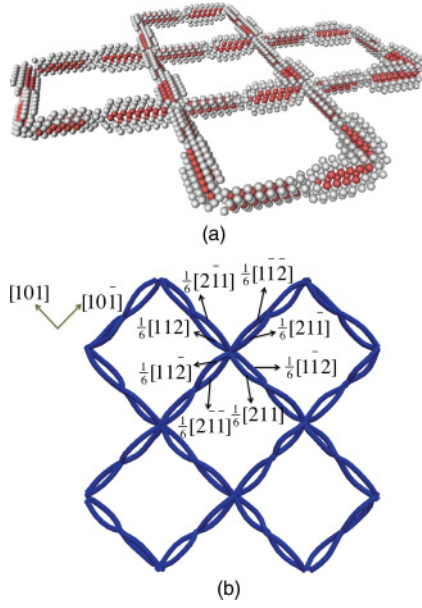


FIG. 1. (Color online) Interface configuration of a (010) TB in fcc Cu. (a) Atomic structure (Ref. 18). Only non-fcc atoms according to the common neighbor analysis are shown [white atoms have unknown structure, while red (grey) atoms have hcp structure]. (b) Dislocation configuration as given by the DXA (Ref. 17) from MD data. Burgers vectors for the partial dislocations and line directions are also presented.

the constrictions in the segments between MDIs remain stable, because in this case the dislocation interactions are well balanced.

To study the relative stability of the constriction, we have investigated three different configurations involving two MDIs. The first configuration has the constriction; the second one has no constrictions and is fully asymmetric with respect to the Burgers vectors, alternating the $\{111\}$ splitting plane in the $[101]$ and $[10\bar{1}]$ directions; and the third one has splitting on the same $\{111\}$ plane for all segments aligned along the $[10\bar{1}]$ direction and on different $\{111\}$ planes for the $[101]$ direction (see Fig. 3). We have calculated (Table I) the elastic and stacking-fault energies for these three configurations. The elastic energy was calculated using the nonsingular formulation of Ref. 20 and includes the dislocation core parametrization of Ref. 19.

The configuration with the constriction has 2.5 eV less energy than the asymmetric configuration and 7.73 eV less energy than the parallel configuration. Also, with no constrictions, splitting on the same $\{111\}$ plane has significantly more energy than on alternating planes.

Two energy terms are responsible for the formation of these constrictions. One is the difference in line tension of screw and edge components: By having the constriction, the partials arriving at the MDIs have their dislocation lines closely aligned with their Burgers vectors, enhancing their screw character, which is energetically beneficial according to linear elasticity²¹ and usually also to anisotropic elasticity, certainly holding true for Cu.

However, to achieve that configuration at both MDIs, a constriction has to be created. At this constriction, the Burgers

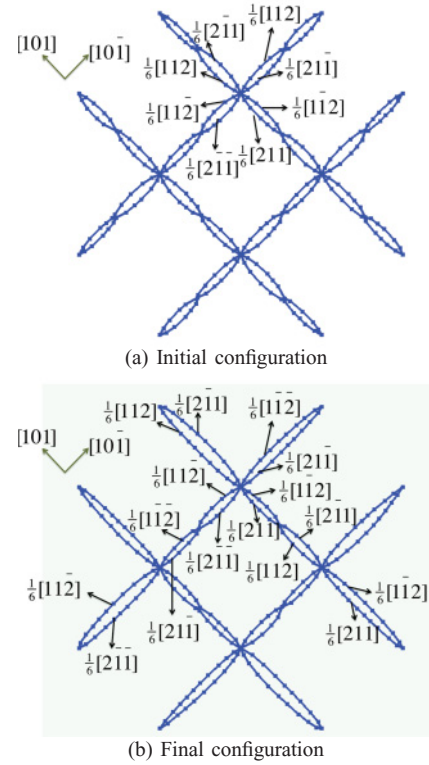


FIG. 2. (Color online) Dislocation configuration of a (010) TB in Cu, as given by DD. Burgers vectors and line directions are also shown.

vectors of the meeting partials oppose the alignment criterion. One might think that these two effects cancel each other, giving no net benefit to the creation of the constriction. The fact that DD indicates a net energy gain reflects the influence of another term: the interaction between the dislocations at the MDIs, where eight partials meet, compared to the interaction at the constrictions, where only four partials meet.

Misfit dislocation intersections and constrictions are preferential sites for heterogeneous nucleation of voids and helium bubbles. To analyze their behavior as sinks we have first studied the interaction energy between the TB and one vacancy, defined as

$$E_{X-TB}^{\text{int}} = E[X-TB] + E[\text{Cu}] - \{E[\text{TB}] + E[X]\}, \quad (1)$$

where X stands for the vacancy, $E[X-TB]$ is the energy of the system with the vacancy and the TB, $E[\text{Cu}]$ is the energy of bulk Cu, $E[\text{TB}]$ is the energy of the system with the TB, and $E[X]$ is the energy of the Cu system with one vacancy. The interaction energy at the MDI is approximately -0.4 eV, while close to the constriction it is approximately -0.53 eV. This difference highlights the tendency for the vacancies to segregate to the constrictions rather than to the MDIs.

Moreover, Fig. 4(a) shows that the energy basin at the MDI is narrower than at the constriction, so possibly more vacancies will be captured by the constriction rather than by the MDI. To test this possibility, we have studied the vacancy accumulation at the interface using an on-the-fly off-lattice kinetic Monte Carlo (KMC) approach.²² Vacancies are considered localized and are introduced at a certain dose rate described below. The rates for vacancy diffusion are obtained from migration

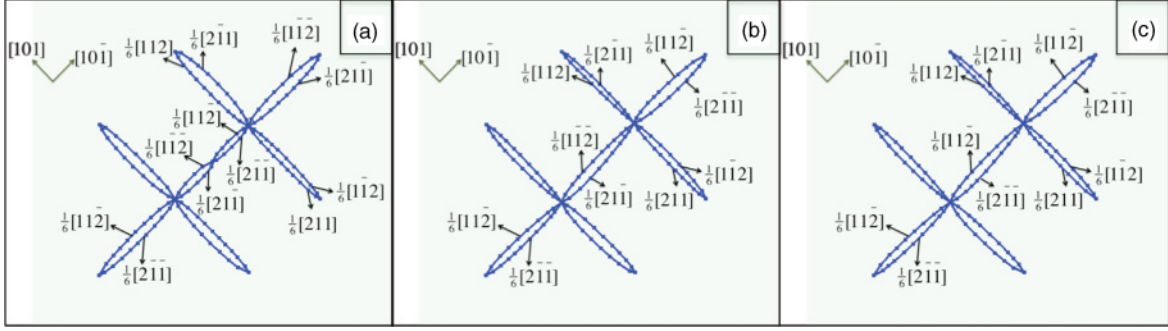


FIG. 3. (Color online) Configurations for two free MDIs in DD. Partial dislocation Burgers vectors and line directions are also shown. (a) Dislocation constriction, (b) asymmetric splitting plane at different sides of the free MDIs, and (c) same splitting plane at different sides of the free MDIs in the $[10\bar{1}]$ direction and different splitting in the $[101]$ direction.

barriers that include atomic relaxation. The migration energy is calculated with a heuristic linear formulation

$$\Delta E_j^{\text{sp}} = E_0 + \frac{E_f - E_i}{2}, \quad (2)$$

where E_0 is the value for the barrier in bulk, E_i is the energy of the initial configuration, and E_f is the energy of the final configuration. These energies are calculated in a relaxed region around the vacancy defined by an adjustable cutoff; here this active volume contains around 1000 atoms. The value for E_0 is taken from *ab initio* calculations; we have used 0.64 eV for fcc Cu.²³ From the migration energy values we calculate the rates following harmonic transition state theory:²⁴

$$\Gamma_\mu = \Gamma_{i \rightarrow j} = \omega_D^\alpha \exp \left\{ -\Delta E_j^{\text{sp}} / kT \right\}, \quad (3)$$

where ω_D^α is taken as the Debye frequency of the hopping atom. We follow the KMC algorithm to exchange the vacancy with a first-nearest-neighbor atom with the right probability, then relax the whole sample following a conjugate gradient algorithm, and update the rates of the vacancy that performed the last hop and its neighboring ones that sit within a defined cutoff (7 Å after convergence). This algorithm follows the methodology of Mason *et al.*^{25,26} The details of the algorithm are given elsewhere.²²

We have inserted vacancies at different rates, from 10^{-1} to 10^2 V/Å³ s, at 500 K. The results are shown in Fig. 5. For low insertion rate vacancies accumulate as voids at the dislocation constrictions, suggesting that vacancies have time to diffuse to those sites before reacting among themselves. With increasing insertion rate ($\geq 10^2$ V/Å³ s), vacancies start to agglomerate at dislocation cores and even in bulk.

TABLE I. Energies for the three different configurations: a system with the constriction, a system asymmetric in the Burgers vector, and a system parallel in the Burgers vector (see Fig. 3). The elastic energy (E_{elas}), stacking-fault energy (E_{SF}), the total energy (E_T) and their increments with respect to the most stable configuration (C) are reported.

Configuration	E_{elas} (eV)	E_{SF} (eV)	E_T (eV)	$E_{A,P} - E_C$
constriction (C)	95.89	21.02	116.91	
asymmetric (A)	98.15	21.30	119.45	2.54
parallel (P)	103.34	21.30	124.64	7.73

We analyze now the implications of this result for the simultaneous production and diffusion of He and vacancies. Helium is produced under irradiation via the (n, α) reaction, most probably as a highly mobile interstitial. Vacancies are produced by the recoil of atoms hit by neutrons or those recoiling from the α decay. Usually many more vacancies than He atoms are produced, so there is a high probability for both to react, making He a much less mobile substitutional defect. To test the tendency of He to segregate to the interface we have calculated its interaction energy with the TB, defined

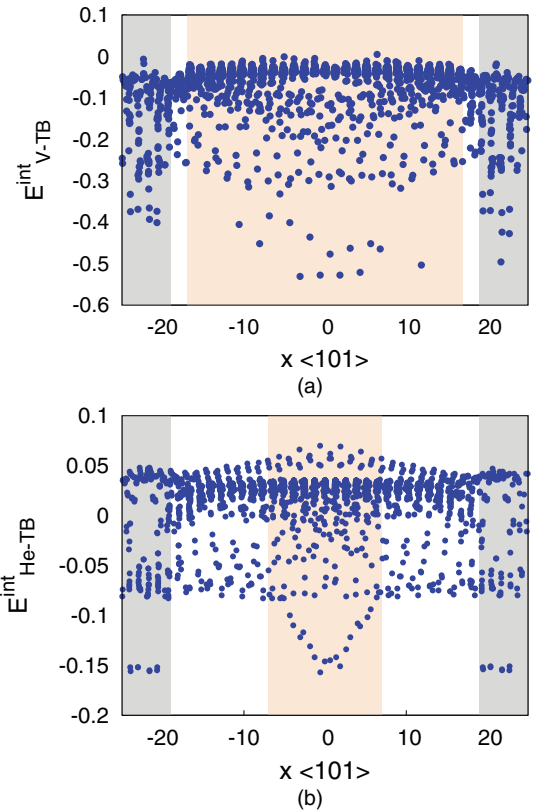


FIG. 4. (Color online) Interaction energy at each atomic position of a 2° {010} Cu TB with (a) a vacancy and (b) a substitutional He atom. The X axis is along the dislocation line between two MDIs. Shaded regions show the approximate width of the MDI basins (grey, edges) and constriction basin [light brown (light grey), center].

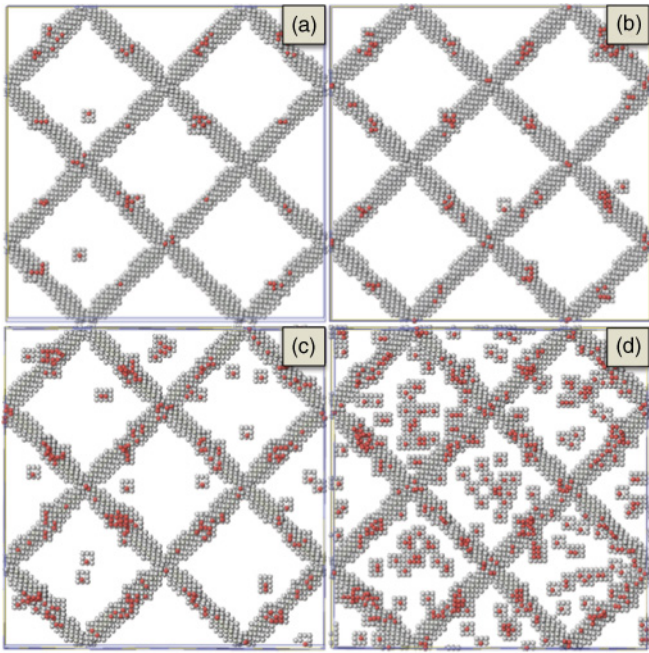


FIG. 5. (Color online) Vacancies [in red (grey)] diffusing toward the TB (in white) at four different production rates: (a) 10^{-1} , (b) 10^0 , (c) 10^1 , and (d) 10^2 V/Å³ s at 500 K. For the low production rate vacancies show a tendency to create voids at the dislocation constrictions, while for higher rates they also precipitate at MDIs, dislocation cores, and in bulk.

as in Eq. (2), where X now stands for substitutional He. We have used the Cu-He interatomic potential developed in Ref. 27. The results in Fig. 4(b) show that the attraction of

the He to constrictions is comparable to its attraction to MDIs (-0.15 eV). The basin of attraction to the constriction seems to be narrower than for vacancies, which might reduce the tendency for substitutional He compared to that of vacancies to segregate to the constrictions. In a general sense, constrictions would enhance the tendency for defects to accumulate at the interface, thus promoting their recombination.

Recent experiments on a TB interface in Au (Ref. 13) show the formation of He bubbles at MDIs. These experiments featured samples with a misorientation angle $\approx 1^\circ$ and a dislocation spacing of 15 nm. According to our DD calculations, at this spacing (and up to 24 nm) the formation of constrictions is again favorable. Unfortunately, the resolution of the transmission electron microscopy analysis does not clarify whether or not constrictions occur in the sample. The extended well of the constriction basin may promote elongated precipitates that are not accessible to the experimental resolution or perhaps the narrower basin for He at the constriction and the stronger attraction to the MDIs reinforces He segregation to the later. In contrast, since the stacking-fault energy is lower in Au than in Cu, the energetic balance may change in favor of the configuration without constriction. In any case, our results call for additional experimental efforts to elucidate the role that constrictions may play in the design of radiation-resistant materials.

This work was performed with support from the Center for Materials at Irradiation and Mechanical Extremes, an Energy Frontier Research Center funded by the US Department of Energy (Grant No. 2008LANL1026) at Los Alamos National Laboratory. A.C. also acknowledges support from the Laboratory Directed Research and Development Program.

*enriquem@lanl.gov

¹B. N. Singh, *Philos. Mag.* **29**, 25 (1974).

²A. H. King and D. A. Smith, *Philos. Mag. A* **42**, 495 (1980).

³M. Demkowicz, P. Bellon, and B. Wirth, *MRS Bull.* **35**, 1 (2010).

⁴R. W. Siegel, S. M. Chang, and R. W. Balluffi, *Acta Metall.* **28**, 249 (1980).

⁵Y. Mishin, C. Herzig, J. Bernardini, and W. Gust, *Inter. Mater. Rev.* **42**, 155 (1997).

⁶R. G. Hoagland, T. E. Mitchell, J. P. Hirth, and H. Kung, *Philos. Mag. A* **82**, 643 (2002).

⁷M. Samaras, P. M. Derlet, H. Van Swygenhoven, and M. Victoria, *Phys. Rev. Lett.* **88**, 125505 (2002).

⁸M. Samaras, P. M. Derlet, H. Van Swygenhoven, and M. Victoria, *J. Nucl. Mater.* **351**, 47 (2006).

⁹E. M. Bringa, J. D. Monk, A. Caro, A. Misra, L. Zepeda-Ruiz, M. Duchaineau, F. Abraham, M. Nastasi, S. T. Picraux, Y. Q. Wang, and D. Farkas, *Nano Lett.* (2011); doi:10.1021/nl201383u.

¹⁰M. Nomura, S.-Y. Lee, and J. B. Adams, *J. Mater. Res.* **1**, 1 (1991).

¹¹M. Nomura and J. B. Adams, *J. Mater. Res.* **7**, 3202 (1992).

¹²X. Liu, X. You, Z. Liu, J. Nie, and Z. Zhuang, *J. Phys. D: Appl. Phys.* **42**, 035404 (2009).

¹³Z. Di, X.-M. Bai, Q. Wei, J. Won, R. G. Hoagland, Y. Wang, A. Misra, B. P. Uberuaga, and M. Nastasi, *Phys. Rev. B* **84**, 052101 (2011).

¹⁴S. M. Foiles, *Phys. Rev. B* **40**, 11502 (1989).

¹⁵S. Plimpton, *J. Comput. Phys.* **117**, 1 (1995).

¹⁶Y. Mishin, M. J. Mehl, D. A. Papaconstantopoulos, A. F. Voter, and J. D. Kress, *Phys. Rev. B* **63**, 224106 (2001).

¹⁷A. Stukowski and K. Albe, *Modell. Simul. Mater. Sci. Eng.* **18**, 085001 (2010).

¹⁸A. Stukowski, *Modell. Simul. Mater. Sci. Eng.* **18**, 015012 (2010).

¹⁹E. Martinez, J. Marian, A. Arsenlis, M. Victoria, and J. M. Perlado, *J. Mech. Phys. Solids* **56**, 869 (2008).

²⁰W. Cai, A. Arsenlis, C. R. Weinberger, and V. V. Bulatov, *J. Mech. Phys. Solids* **54**, 561 (2006).

²¹J. P. Hirth and J. Lothe, *Theory of Dislocations* (Krieger, Malabar, Florida, 1992).

²²E. Martinez, J. Hetherly, M. Nastasi, and A. Caro (unpublished).

²³F. Soisson and C.-C. Fu, *Phys. Rev. B* **76**, 214102 (2007).

²⁴G. H. Vineyard, *J. Phys. Chem. Solids* **3**, 121 (1957).

²⁵D. R. Mason, R. E. Rudd, and A. P. Sutton, *J. Phys. Condens. Matter* **16**, 2679 (2004).

²⁶D. R. Mason, R. E. Rudd, and A. P. Sutton, *Comput. Phys. Commun.* **160**, 140 (2004).

²⁷A. Kashinath and M. J. Demkowicz, *Modell. Simul. Mater. Sci. Eng.* **19**, 035007 (2011).